Measurement of valence-band offset at native oxide/$BaSi_2$ interfaces by hard x-ray photoelectron spectroscopy

Ryota Takabe,[1] Weijie Du,[1] Keita Ito,[1,2,3] Hiroki Takeuchi,[1] Kaoru Toko,[1] Shigenori Ueda,[4,5] Akio Kimura,[6] and Takashi Suemasu[1,7]
[1]*Institute of Applied Physics, University of Tsukuba, Tsukuba, Ibaraki 305-8573, Japan*
[2]*Japan Society for the Promotion of Science (JSPS), Chiyoda, Tokyo 102-0083, Japan*
[3]*Department of Electronic Engineering, Graduate School of Engineering, Tohoku University, Sendai 980-8579, Japan*
[4]*Synchrotron X-ray Station at SPring-8, National Institute for Materials Science (NIMS), Hyogo 679-5148, Japan*
[5]*Quantum Beam Unit, NIMS, Tsukuba, Ibaraki 305-0047, Japan*
[6]*Graduate School of Science, Hiroshima University, Higashi-hiroshima 739-8526, Japan*
[7]*Japan Science and Technology Agency, CREST, Tokyo 102-0075, Japan*

(Received 14 October 2015; accepted 24 December 2015; published online 13 January 2016)

Undoped n-type $BaSi_2$ films were grown on Si(111) by molecular beam epitaxy, and the valence band (VB) offset at the interface between the $BaSi_2$ and its native oxide was measured by hard x-ray photoelectron spectroscopy (HAXPES) at room temperature. HAXPES enabled us to investigate the electronic states of the buried $BaSi_2$ layer non-destructively thanks to its large analysis depth. We performed the depth-analysis by varying the take-off angle (TOA) of photoelectrons as 15°, 30°, and 90° with respect to the sample surface and succeeded to obtain the VB spectra of the $BaSi_2$ and the native oxide separately. The VB maximum was located at −1.0 eV from the Fermi energy for the $BaSi_2$ and −4.9 eV for the native oxide. We found that the band bending did not occur near the native oxide/$BaSi_2$ interface. This result was clarified by the fact that the core-level emission peaks did not shift regardless of TOA (i.e., analysis depth). Thus, the barrier height of the native oxide for the minority-carriers in the undoped n-$BaSi_2$ (holes) was determined to be 3.9 eV. No band bending in the $BaSi_2$ close to the interface also suggests that the large minority-carrier lifetime in undoped n-$BaSi_2$ films capped with native oxide is attributed not to the band bending in the $BaSi_2$, which pushes away photogenerated minority carriers from the defective surface region, but to the decrease of defective states by the native oxide. © *2016 AIP Publishing LLC*.
[http://dx.doi.org/10.1063/1.4939614]

I. INTRODUCTION

Thin-film solar cells composed of Cu(In,Ga)Se_2 (CIGS) and CdTe have yielded practical applications because of their high energy conversion efficiency and low cost.[1–6] These materials include toxic and/or not-abundant metal elements. Therefore, materials consisting of earth-abundant and environmental-friendly elements are preferable. To realize such thin-film solar cells, Si thin-film solar cells have been studied extensively;[7–12] however, it is not easy to achieve high efficiency as large as 20% because the absorption coefficient of crystalline Si is much smaller than that of CIGS. It is thereby very important to explore other thin-film solar cell materials composed of non-toxic and earth abundant elements. Among such materials, we have focused much attention on semiconducting barium disilicide ($BaSi_2$). $BaSi_2$ has a band gap of approximately 1.3 eV, matching the solar spectrum.[13,14] In addition, it has a large absorption coefficient reaching $3 \times 10^4\,cm^{-1}$ at 1.5 eV,[14] which might enable us to achieve high-efficiency thin-film solar cells. Besides, minority-carrier diffusion length (ca. 10 μm)[15] and minority-carrier lifetime, τ, (ca. 14 μs)[16,17] of undoped n-$BaSi_2$ are sufficiently large for thin-film solar cell application. Our previous studies suggested that the native oxide layer on the surface of undoped n-$BaSi_2$ acts as a passivation layer; τ reached approximately 10 μs.[18] According to the previous x-ray photoelectron spectroscopy (XPS) studies, we found that this native oxide layer was composed of oxides such as SiO_x and $BaCO_3$.[18] But we could not discuss how the native oxides contribute to the surface passivation due to the lack of depth-dependent analysis for the native oxide/n-$BaSi_2$ heterostructure. In addition, we have recently achieved the solar cell operation in the devices utilizing the native oxide/n-$BaSi_2$ heterointerface.[19] The efficiency was quite limited because the transport of photogenerated minority carriers (holes) was blocked by the native oxide. In order to improve the device performance, extraction of the photogenerated holes more efficiently through the native oxide layer via tunneling is needed. At present, the barrier height of the native oxide for holes is unknown. Hard x-ray photoelectron spectroscopy (HAXPES) is a powerful tool as a direct probe of valence band (VB) density of states (DOS) of $BaSi_2$ under its native oxide. This is because the analysis-depth of HAXPES is much deeper than that of conventional XPS and ultraviolet photoelectron spectroscopy.[20–29] In general, conventional XPS in the electron kinetic-energy range of 50–100 eV is quite surface sensitive due to the short electron inelastic mean free path (IMFP), λ, of <5 Å. The conventional XPS spectra strongly reflect electronic states at surfaces of solids,

which make it difficult to examine the electronic states inside the solids. Although the larger probing depth than 50 Å could be expected for HAXPES, a significantly reduced photoionization cross-section prevented us from measuring VB photoelectron spectra above 3 keV.[30,31] An extremely brilliant X-ray provided from the third generation synchrotron source can well compensate for the diminished cross section and has enabled us to perform HAXPES measurements with high-energy resolution.[32] There have been several reports utilizing this large probing depth on the measurement of VB spectra of buried layers such as CdS/Cu_2ZnSnS_4 (CZTS), AlO_x/Si heterostructures, and Bi_2Se_3 surface.[20–22] For example, in Ref. 20, CdS/CZTS heterostructures formed on Mo-coated glass, where the CdS layer thickness was varied as 0, 5, and 100 nm, were examined by changing the effective IMFP, which was controlled by take-off angle (TOA) of photoelectrons in HAXPES. Consequently, they succeeded to measure the VB spectra of CdS and CZTS, separately, and obtained the VB offset (VBO) at the CdS/CZTS interface to be 0.0 ± 0.1 eV in a real device structure. In this study, we have performed the HAXPES measurements for the native oxide/$BaSi_2$ in order to examine the VBO at the interface, and the band bending near the interface.

II. EXPERIMENTAL METHOD

We used an ion-pumped molecular beam epitaxy (MBE) system equipped with standard Knudsen cells for Ba and CaF_2 and an electron-beam evaporation source for Si in this study. The base pressure of the MBE system was less than 10^{-8} Pa. The procedure of the sample preparation is as follows. First, Ba was deposited on a Si(111) substrate at 500 °C to form a 5-nm-thick $BaSi_2$ template layer by reactive deposition epitaxy (RDE).[33] This layer works as a kind of seed crystals for subsequent layers. Next, Ba and Si were co-evaporated on the template layer at 580 °C by MBE to form 600-nm-thick undoped n-$BaSi_2$ epitaxial films.[34,35] After the MBE growth, the sample was exposed to air for 3 min (sample A) and 24 h (sample B) to form a native oxide on the $BaSi_2$ surface, followed by the deposition of a 100-nm-thick ITO layer by radio-frequency magnetron sputtering method at room temperature (RT). For sample C, the $BaSi_2$ surface was exposed to air for 26 h after the MBE growth. For comparison, sample D was prepared, where the $BaSi_2$ film was capped *in situ* with a 2-nm-thick CaF_2 layer in order to prevent the surface oxidation.[36] The oxide layer thicknesses for samples A and B were evaluated by cross-sectional transmission electron microscope (TEM; FEI, Tecnai Osiris) with an acceleration voltage of 200 kV. Thin foils for TEM observation were prepared with a focused ion beam micro-sampling system. The layer structures of samples A–D are summarized in Table I.

HAXPES measurements were performed at the revolver undulator beamline BL15XU[32,37] of SPring-8 in Japan. The excitation photon energy was set to 5953 eV, and the incident angle of the photon was set to ca. 2°–5° with respect to the sample surface. The TOA dependence of HAXPES measured at 15°, 30°, and 90° with respect to the sample surface was performed at RT. The overall energy resolution was set to 150 meV. The Fermi energy, E_F, was referred to the Fermi cut-off of an evaporated Au film.

TABLE I. Sample preparation: $BaSi_2$ layer thickness, air exposure duration, native oxide thickness, and surface capping, and its layer thickness are specified.

Sample	$BaSi_2$ layer (nm)	Air exposure duration	Native oxide (nm)	Capping (nm)
A	600	3 min	6	100 (ITO)
B	600	24 h	8	100 (ITO)
C	600	26 h	ca. 8	0
D	35	0	0	2 (CaF_2)

III. RESULTS AND DISCUSSION

Figures 1(a) and 1(b) show the bright-field cross-sectional TEM images and the selected area diffraction (SAD) patterns of samples A and B, respectively. As shown in the SAD patterns, diffraction spots corresponding to (200), (400), and (600) planes of $BaSi_2$ are aligned normal to the sample surface, thereby we succeeded to grow the *a*-axis-oriented $BaSi_2$ epitaxial films on Si(111). The native oxide layer thickness is approximately 6 nm in sample A and 8 nm in sample B. The difference between them is small although the air exposure duration is quite different, that is, 3 min for sample A and 24 h for sample B. This means that the native oxide layer formed in a short period of time, and its layer thickness almost saturated after 24 h. Therefore, it is reasonable to suppose the native oxide layer thickness in sample C, used for HAXPES measurements, to be also approximately 8 nm. Regarding the stability and reproducibility of the native oxide, it was found from the secondary ion mass spectrometry measured on samples more than one month after their growth that a large concentration of O atoms ($\sim 10^{22}$ cm^{-3}) existed only in the region close to the samples surface like in samples A and B. We can thereby safely state that the native oxide is stable at least on a $BaSi_2$ epitaxial film during such period.

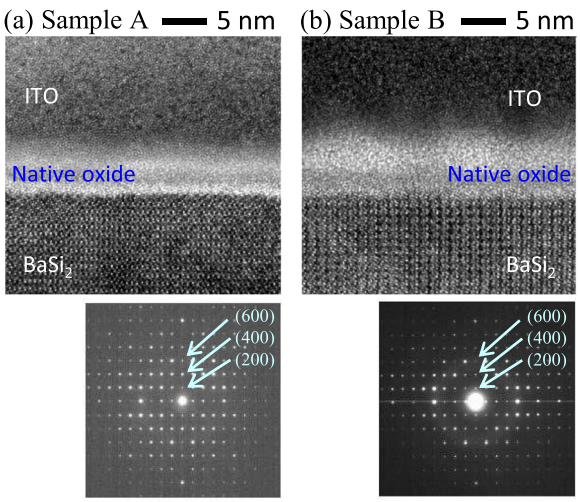

FIG. 1. Cross-sectional TEM and SAD images of (a) ITO(100 nm)/oxide (6 nm)/$BaSi_2$(600 nm) (sample A) and (b) ITO(100 nm)/oxide(8 nm)/$BaSi_2$(600 nm) (sample B).

Figure 2 shows the wide range HAXPES spectra of (a) sample C and (b) sample D[36] taken at TOA = 90°. In the figures, we can see the intense peaks of the Ba and Si core-levels. In addition, the O 1*s* core-level peak was also observed in sample C as seen in Fig. 2(a). On the other hand, the O 1*s* core-level peak was negligibly weak in sample D, which was $BaSi_2$ capped *in situ* with CaF_2,[36] in Fig. 2(b).

Figure 3(a) shows the expected spectrum, which is the sum of the rescaled partial DOSs of Si 3*s*, 3*p*, and Ba 6*s* states using their photo-ionization cross-sections at a photon energy of 6 keV. E_F is located in the middle of the band gap. Calculation details are given in our previous report.[36] The main VB feature of $BaSi_2$ extends from approximately −0.5 eV to −4 eV. The validity of this calculation was proved by the measured VB HAXPES spectrum of sample D in Fig. 3(b), which resembles the calculated VB spectrum in Fig. 3(a). The contribution of the 2-nm-thick CaF_2 capping layer to the VB spectrum was negligible because of the following two reasons: (1) the VB maximum of CaF_2 is located far below that of $BaSi_2$ due to the large band gap (ca. 12 eV), and (2) the spectrum in Fig. 3(b) was not measured under surface-sensitive condition but under bulk-sensitive condition. According to Tanuma-Powell-Penn equation,[38] the IMFP value, λ, was calculated to be approximately 10 nm for $BaSi_2$ at 6 keV. The HAXPES intensity decays as $\exp(-x/\lambda)$ at a depth x beneath the surface, and the photoelectron which contributes to the HAXPES intensity comes from a range of 3λ from the surface. Thus, the probing depth is estimated to be $3\lambda \times \sin(\mathrm{TOA})$, that is, approximately 30 nm for TOA = 90°. This value is much larger than the native oxide layer thickness (ca. 8 nm), and therefore, the HAXPES intensity originating from the $BaSi_2$ becomes pronounced. For these reasons, the contribution of the CaF_2 can be neglected in Fig. 3(b).

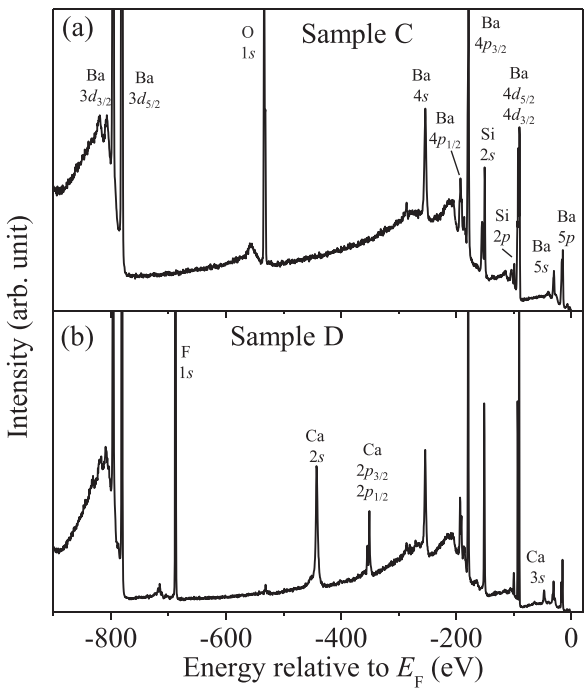

FIG. 2. Wide-range HAXPES spectra of (a) oxide(ca. 8 nm)/$BaSi_2$(600 nm) (sample C) and (b) CaF_2(2 nm)/$BaSi_2$(35 nm) (sample D).[36]

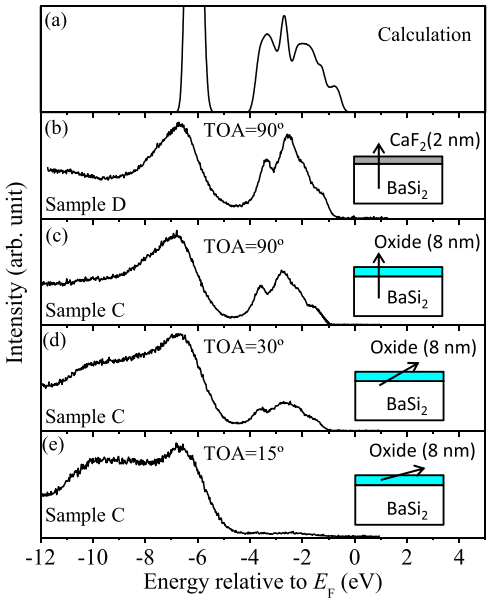

FIG. 3. (a) Calculated spectrum[36] and (b) HAXPES spectrum of CaF_2(2 nm)/$BaSi_2$(35 nm) (sample D).[36] HAXPES spectra of oxide(ca. 8 nm)/$BaSi_2$(600 nm) (sample C) when TOA is (c) 90°, (d) 30°, and (e) 15°. Schematics of sample structure and TOA denoted by arrows are also shown.

Next, we discuss the results on sample C, $BaSi_2$ capped with native oxide. Figures 3(c)–3(e) show the HAXPES spectra measured at TOA = 90°, 30°, and 15°, respectively. The spectrum in Fig. 3(c) was measured under bulk-sensitive condition and that in Fig. 3(e) under surface-sensitive condition. The VB HAXPES spectrum in Fig. 3(c) is quite similar to that in Fig. 3(b). The VB structures originating from the $BaSi_2$ start to increase at approximately −1 eV and extend up to approximately −4 eV in sample C, measured at TOA = 90°. On the other hand, the VB structures are negligibly weak in the above-mentioned energy range at TOA = 15° as shown in Fig. 3(e). We should also note that the VB HAXPES spectrum in Fig. 3(d) is the intermediate one between those in Figs. 3(c) and 3(e). Since the HAXPES spectrum shown in Fig. 3(e) was measured under the surface-sensitive condition of TOA = 15°, it is safe to state that the VB of the native oxide appears dominant in Fig. 3(e).

Figures 4(a) and 4(b), respectively, show the HAXPES spectrum around −1.0 eV in Fig. 3(c), near the VB maximum of $BaSi_2$, E_V^{BaSi2}, and that around −5.0 eV in Fig. 3(e), near the VB maximum of the native oxide, E_V^{oxide}. E_V^{BaSi2} and E_V^{oxide} are derived to be −1.0 and −4.9 eV, respectively, with respect to E_F by means of the linear extrapolation to the baseline as shown in Fig. 4. VBO at the native oxide/$BaSi_2$ is not given just by the difference between E_V^{oxide} and E_V^{BaSi2} because the band bending in the $BaSi_2$ near the interface should be considered. To investigate the influence of this band bending, we next compared the core-level spectra obtained for different TOAs.

Figure 5 shows the Ba $3d_{3/2}$ core-level spectra in sample C at TOA = 15°, 30°, and 90°. Each spectrum is well reconstructed by the sum of two Gaussian curves (broken lines) located at −795.9 eV and −797.1 eV. We attribute the peak at −795.9 eV (−797.1 eV) to the $BaSi_2$ layer (the surface native oxide layer) because of the strong reduction of the

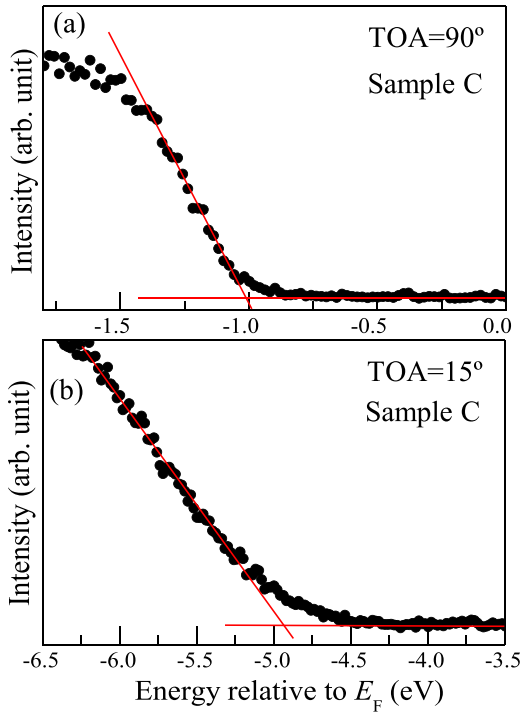

FIG. 4. Enlarged spectra for sample C around (a) −1 eV in Fig. 3(c) and 3(b) −5 eV in Fig. 3(e), corresponding to the HAXPES spectra around the VB maximum of $BaSi_2$ and native oxide, respectively.

peak at −795.9 eV in the surface-sensitive spectrum (TOA = 15°). As seen in Fig. 5, the peak energy positions and shapes did not change regardless of TOA, thereby analyzing depth information. This means that the band bending did not occur or it was negligibly small around the oxide/$BaSi_2$ interface. If there are lot of defects in the $BaSi_2$ close to the interface, E_F pinning is likely to occur there, resulting in the band bending as is often the case with Si,[39] GaAs,[40] and InN.[41] No band bending in the $BaSi_2$ layer indicates that the native oxide/$BaSi_2$ interface is not defective. This is consistent with our previous result.[19] According to Ref. 19, the capacitance versus voltage characteristics of the device structures composed of the native oxide/$BaSi_2$ interface

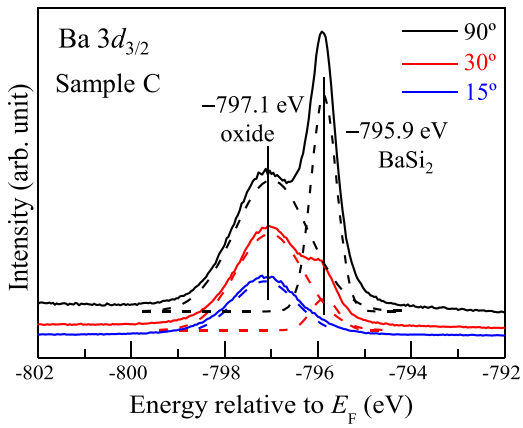

FIG. 5. Ba $3d_{3/2}$ core-level HAXPES spectra for sample C taken at TOA = 15°, 30°, and 90°. Each spectrum can be fitted by the sum of two Gaussian curves (broken lines) peaking at −795.9 eV and −797.1 eV. Broken lines are shifted downward a little to be seen.

revealed that the trapped electrons at the surface defect states decreased with the air exposure duration of the $BaSi_2$ surface. On the basis of these results, the band lineup of the native oxide layer and $BaSi_2$ can be obtained as shown in Fig. 6. We thus conclude that the barrier height of the native oxide layer against holes, minority carriers in n-$BaSi_2$, is approximately 3.9 eV (= 4.9 eV – 1.0 eV).

We next discuss the reason why the minority-carrier lifetime in undoped n-type $BaSi_2$ is improved from ca. 0.2 μs to ca. 10 μs by forming the native oxide on the $BaSi_2$ surface.[18] Surface passivation is widely known in crystalline Si capped with oxides such as SiO_2 and Al_2O_3.[42–48] It is attributed to two mechanisms, that is, the decrease of surface states in Si by terminating the dangling bonds of Si and the electric-field due to charges in the oxides, which bends the energy band of Si near the oxide/Si interface so as the photogenerated minority carriers are pushed away from the defective surface region. In the case of native oxide/$BaSi_2$, such a band bending does not exist as discussed in Fig. 5. It is thus the decrease of the surface states that accounts for the large minority-carrier lifetime obtained for $BaSi_2$ capped with native oxide. Now that the barrier height of holes is made clear, and thinning of the oxide layer thickness with more precision might enhance the transport of photogenerated holes through the native oxide layer via tunneling and improve the solar cell efficiency much further.

IV. SUMMARY

We formed 600-nm-thick *a*-axis-oriented undoped n-$BaSi_2$ epitaxial layers on Si(111) by MBE and directly measured the electronic states of the buried $BaSi_2$ layers under the 8-nm-thick native oxide by HAXPES. We performed the depth-analysis by varying TOA of 15°, 30°, and 90° and obtained the VB spectra of the $BaSi_2$ and the native oxide separately. The VB maximum was located at −4.9 eV from E_F for the native oxide and −1.0 eV for the $BaSi_2$. The VBO at the native oxide/$BaSi_2$ interface, that is, the barrier height for holes in n-$BaSi_2$, was thus determined to be 3.9 eV. The Ba 3*d* core-level HAXPES spectra revealed that there was no band bending in the $BaSi_2$ close to the native oxide/$BaSi_2$ interface. This means that the large minority-carrier lifetime in undoped n-$BaSi_2$ films capped with native

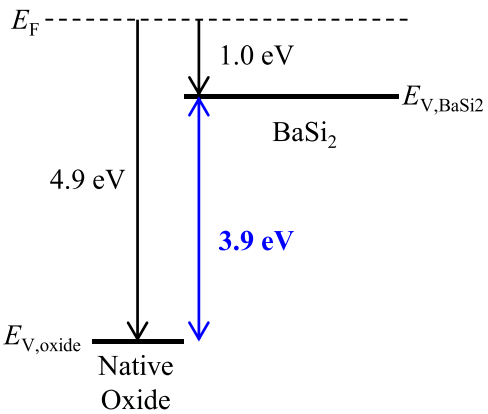

FIG. 6. Band lineup of the native oxide and $BaSi_2$ layers determined by the HAXPES measurements.

oxide is attributed not to the band bending in the $BaSi_2$, which keeps photogenerated minority carriers away from the defective surface region, but to the decrease of defective states by the native oxide.

ACKNOWLEDGMENTS

The HAXPES measurements were performed at Synchrotron X-ray Station of BL15XU, at SPring-8, and were supported by NIMS microstructural characterization platform as a program of "Nanotechnology Platform" (Proposal Nos. 2014A4902 and 2015A4907) of the Ministry of Education, Culture, Sports, Science and Technology (MEXT), Japan. S.U and A.K. are grateful to HiSOR, Hiroshima University and JAEA at SPring-8 for the development of HAXPES at BL15XU. The authors thank Dr. N. Yoshizawa and Mr. N. Saito for their help in TEM observations conducted at the Electron Microscope Facility, supported by the IBEC Innovation Platform, AIST, Japan. This work was financially supported by the Japan Science and Technology Agency (JST/CREST) and by a Grants-in-Aid for Scientific Research A (15H02237) from the Japan Society for the Promotion of Science (JSPS). R.T. was financially supported by Grants-in-Aid for JSPS Fellows (15J02139).

[1]A. Romeo, A. Terheggen, D. Abou-Ras, D. L. Batzner, F. J. Haug, M. Kalin, D. Rudmann, and A. N. Tiwari, Prog. Photovoltaics **12**, 93 (2004).
[2]I. Repins, M. A. Contreras, B. Egaas, C. DeHart, J. Scharf, C. L. Perkins, B. To, and R. Noufi, Prog. Photovoltaics **16**, 235 (2008).
[3]M. A. Green and S. R. Wenham, Appl. Phys. Lett. **65**, 2907 (1994).
[4]H. Katagiri, K. Jimbo, W. S. Maw, K. Oishi, M. Yamazaki, H. Araki, and A. Takeuchi, Thin Solid Films **517**, 2455 (2009).
[5]K. Tanaka, M. Oonuki, N. Moritake, and H. Uchiki, Sol. Energy Mater. Sol. Cells **93**, 583 (2009).
[6]W. W. Yu, L. Qu, W. Guo, and X. Peng, Chem. Mater. **15**, 2854 (2003).
[7]H. Sasaki, H. Morikawa, Y. Matsuno, M. Deguchi, T. Ishihara, H. Kumabe, T. Murotani, and S. Mitsui, Jpn. J. Appl. Phys., Part 1 **33**, 3389 (1994).
[8]J. Meier, S. Dubail, R. Platz, P. Torres, U. Kroll, J. A. A. Selvan, N. P. Vaucher, Ch. Hof, D. Fischer, H. Keppner, R. Flückiger, A. Shah, V. Shklover, and K.-D. Ufert, Sol. Energy Mater. Sol. Cells **49**, 35 (1997).
[9]O. Vetterl, F. Finger, R. Carius, P. Hapke, L. Houben, O. Kluth, A. Lambertz, A. Mück, B. Rech, and H. Wagner, Sol. Energy Mater. Sol. Cells **62**, 97 (2000).
[10]J. Müller, B. Rech, J. Springer, and M. Vanecek, Sol. Energy **77**, 917 (2004).
[11]A. V. Shah, H. Schade, M. Vanecek, J. Meier, E. Vallat-Sauvain, N. Wyrsch, U. Kroll, C. Droz, and J. Bailat, Prog. Photovoltaics **12**, 113 (2004).
[12]P. Bermel, C. Luo, L. Zeng, L. C. Kimerling, and J. D. Joannopoulus, Opt. Express **15**, 16986 (2007).
[13]K. Morita, Y. Inomata, and T. Suemasu, Thin Solid Films **508**, 363 (2006).
[14]K. Toh, T. Saito, and T. Suemasu, Jpn. J. Appl. Phys., Part 1 **50**, 068001 (2011).
[15]M. Baba, K. Toh, K. Toko, N. Saito, N. Yoshizawa, K. Jiptner, T. Sakiguchi, K. O. Hara, N. Usami, and T. Suemasu, J. Cryst. Growth **348**, 75 (2012).
[16]K. O. Hara, N. Usami, K. Toh, M. Baba, K. Toko, and T. Suemasu, J. Appl. Phys. **112**, 083108 (2012).
[17]K. O. Hara, N. Usami, K. Nakamura, R. Takabe, M. Baba, K. Toko, and T. Suemasu, Appl. Phys. Express **6**, 112302 (2013).
[18]R. Takabe, K. O. Hara, M. Baba, W. Du, N. Shimada, K. Toko, N. Usami, and T. Suemasu, J. Appl. Phys. **115**, 193510 (2014).
[19]W. Du, R. Takabe, M. Baba, H. Takeuchi, K. O. Hara, K. Toko, N. Usami, and T. Suemasu, Appl. Phys. Lett. **106**, 122104 (2015).
[20]S. Tajima, K. Kataoka, N. Takahashi, Y. Kimoto, T. Fukano, M. Hasegawa, and H. Hazama, Appl. Phys. Lett. **103**, 243906 (2013).
[21]N. Ikeno, Y. Yamashita, H. Oji, S. Miki, K. Arafune, H. Yoshida, S. Satoh, I. Hirosawa, T. Chikyow, and A. Ogura, Jpn. J. Appl. Phys., Part 1 **54**, 08KD19 (2015).
[22]C. E. ViolBarbosa, C. Shekhar, B. Yan, S. Ouardi, E. Ikenaga, G. H. Fecher, and C. Felser, Phys. Rev. B **88**, 195128 (2013).
[23]M. Sowinska, T. Bertaud, D. Walczyk, S. Thiess, M. A. Schubert, M. Lukosius, W. Drube, Ch. Walczyk, and T. Schoeder, Appl. Phys. Lett. **100**, 233509 (2012).
[24]J. Rubio-Zuazo and G. R. Castro, Surf. Interface Anal. **40**, 1438 (2008).
[25]R. Claessen, M. Sing, M. Paul, G. Berner, A. Wetscherek, A. Müller, and W. Drube, New J. Phys. **11**, 125007 (2009).
[26]G. Panaccione and K. Kobayashi, Surf. Sci. **606**, 125 (2012).
[27]T. Nagata, S. Oh, Y. Yamashita, H. Yoshikawa, N. Ikeno, K. Kobayashi, T. Chikyow, and Y. Wakayama, Appl. Phys. Lett. **102**, 043302 (2013).
[28]L. A. Walsh, G. Hughes, P. K. Hurley, J. Lin, and J. C. Woicik, Appl. Phys. Lett. **101**, 241602 (2012).
[29]D. Gerlach, R. G. Wilks, D. Wippler, M. Wimmer, M. Lozac'h, R. Félix, A. Mück, M. Meier, S. Ueda, H. Yoshikawa, M. Gorgoi, K. Lips, B. Rech, M. Sumiya, J. Hüpkes, K. Kobayashi, and M. Bär, Appl. Phys. Lett. **103**, 023903 (2013).
[30]M. B. Trzhaskovskaya, V. I. Nefedov, and V. G. Yarzhemsky, At. Data Nucl. Data Tables **77**, 97 (2001).
[31]M. B. Trzhaskovskaya, V. I. Nefedov, and V. G. Yarzhemsky, At. Data Nucl. Data Tables **82**, 257 (2002).
[32]S. Ueda, Y. Katsuya, M. Tanaka, H. Yoshikawa, Y. Yamashita, S. Ishimaru, Y. Matsushita, and K. Kobayashi, AIP Conf. Proc. **1234**, 403 (2010).
[33]Y. Inomata, T. Nakamura, T. Suemasu, and F. Hasegawa, Jpn. J. Appl. Phys., Part 1 **43**, 4155 (2004).
[34]Y. Inomata, T. Nakamura, T. Suemasu, and F. Hasegawa, Jpn. J. Appl. Phys., Part 2 **43**, L478 (2004).
[35]R. Takabe, K. Nakamura, M. Baba, W. Du, M. A. Khan, K. Toko, M. Sasase, K. O. Hara, N. Usami, and T. Suemasu, Jpn. J. Appl. Phys. **53**, 04ER04 (2014).
[36]M. Baba, K. Ito, W. Du, T. Sanai, K. Okamoto, K. Toko, S. Ueda, Y. Imai, A. Kimura, and T. Suemasu, J. Appl. Phys. **114**, 123702 (2013).
[37]S. Ueda, J. Electron Spectrosc. Rel. Phenom. **190**, 235 (2013).
[38]S. Tanuma, C. J. Powell, and D. R. Penn, Surf. Interface Anal. **43**, 689 (2011).
[39]F. J. Himpsel, G. Hollinger, and R. A. Pollak, Phys. Rev. B **28**, 7014 (1983).
[40]H. Hasegawa, H. Ishi, T. Sawada, T. Saitoh, S. Konishi, Y. Liu, and H. Ohno, J. Vac. Technol. B **6**, 1184 (1988).
[41]I. Mahboob, T. D. Veal, C. F. McConville, H. Lu, and W. J. Schaff, Phys. Rev. Lett. **92**, 036804 (2004).
[42]A. G. Aberle, S. Glunz, and W. Warta, J. Appl. Phys. **71**, 4422 (1992).
[43]A. W. Stephens, A. G. Aberle, and M. A. Green, J. Appl. Phys. **76**, 363 (1994).
[44]S. W. Glunz, A. B. Sproul, W. Warta, and W. Wettling, J. Appl. Phys. **75**, 1611 (1994).
[45]H. Kobayashi, A. Asano, S. Asada, T. Kubota, Y. Yamashita, K. Yoneda, and Y. Todoroki, J. Appl. Phys. **83**, 2098 (1998).
[46]A. G. Aberle, Prog. Photovoltaics **8**, 473 (2000).
[47]B. Hoex, S. B. S. Heil, E. Langereis, M. C. M. van de Sanden, and W. M. M. Kessels, Appl. Phys. Lett. **89**, 042112 (2006).
[48]J. Schmidt, A. Merkle, R. Brendel, B. Hoex, M. C. M. van de Sanden, and W. M. M. Kessels, Prog. Photovoltaics **16**, 461 (2008).